



Deposited via The University of Sheffield.

White Rose Research Online URL for this paper:

<https://eprints.whiterose.ac.uk/id/eprint/204038/>

Version: Published Version

---

**Proceedings Paper:**

Schiantella, M., Gilbert, M., Smith, C. et al. (2022) Limit analysis of non-periodic masonry by means of discontinuity layout optimization. In: 8th European Congress on Computational Methods in Applied Sciences and Engineering. 8th European Congress on Computational Methods in Applied Sciences and Engineering, 05-09 Jun 2022, Oslo, Norway. CIMNE. ISBN: 9788412322286. EISSN: 2696-6999.

<https://doi.org/10.23967/eccomas.2022.168>

---

**Reuse**

This article is distributed under the terms of the Creative Commons Attribution-NonCommercial-ShareAlike (CC BY-NC-SA) licence. This licence allows you to remix, tweak, and build upon this work non-commercially, as long as you credit the authors and license your new creations under the identical terms. More information and the full terms of the licence here: <https://creativecommons.org/licenses/>

**Takedown**

If you consider content in White Rose Research Online to be in breach of UK law, please notify us by emailing [eprints@whiterose.ac.uk](mailto:eprints@whiterose.ac.uk) including the URL of the record and the reason for the withdrawal request.

# LIMIT ANALYSIS OF NON-PERIODIC MASONRY BY MEANS OF DISCONTINUITY LAYOUT OPTIMIZATION

Mattia Schiantella<sup>1</sup>, Matthew Gilbert<sup>2</sup>, Colin C. Smith<sup>2</sup>, Linwei He<sup>2</sup>, Federico Cluni<sup>1</sup>,  
Vittorio Gusella<sup>1</sup>

<sup>1</sup> Dept. Civil and Environmental Engineering, University of Perugia, via G.Duranti 93,  
mattia.schiantella@studenti.unipg.it, {federico.cluni, vittorio.gusella}@unipg.it

<sup>2</sup> Dept. Civil and Structural Engineering, University of Sheffield, Mappin Street S1 3JD,  
{m.gilbert, c.c.smith, linwei.he}@sheffield.ac.uk

**Key words:** Limit analysis, Non-periodic masonry, Discontinuity Layout Optimization

**Abstract.** Masonry structures forming part of our historical heritage were often constructed using non-periodic textures. In this case, unlike the situation for masonry with periodic textures, few methods are available to estimate wall strength and, moreover, available methods are often difficult to apply. In this work, Discontinuity Layout Optimization (DLO) is proposed as a method of estimating the failure load and associated mechanism of masonry walls constructed with non-periodic textures. In the first part three different textures are considered (periodic, quasi-periodic and chaotic) with a simplified scheme and a parametric analysis is undertaken, considering the variation of the height of the panel. A further classification for quasi-periodic textures is then provided and a DLO rigid block analysis is carried for square panels to show the influence of such textures. The results highlight the importance of the parameters considered in the analysis, and that DLO is a suitable method to investigate their influence.

## 1 INTRODUCTION

Historical masonry walls were often built using irregular textures. In the worst case scenario their interior also includes rubble or earth so they are subject to disaggregation, though this case will not be considered in here. A texture is ‘periodic’ if it is characterized by blocks arranged in a regular pattern, as shown in Figure 1 (a). In this case the position of each block is given by a linear combination of two vectors (indicated by  $v_1$  and  $v_2$  in the figure)

For non-periodic masonry textures, we define two different typologies. The quasi-periodic texture [1], is given by blocks of different size but arranged in such a way that courses of a given height are present, and so the horizontal mortar joints are almost aligned, as shown in Figure 1 (b). The second non-periodic texture is the chaotic texture, in which blocks of different size can be arranged arbitrarily; moreover, the blocks will often have non rectangular shapes (see Figure 1 (c)).

It is possible to model a masonry structure both with a discrete or a smeared continuum approach. In the first case, masonry elements are modelled explicitly and this allows the non-periodicity to be represented directly, with masonry joints assumed to have zero thickness. Some examples of this approach are [2], [3], [4] and [5], where in the latter two works non-associative friction was considered. A drawback of this approach is that if the structure comprises of many units, it can be computationally expensive.

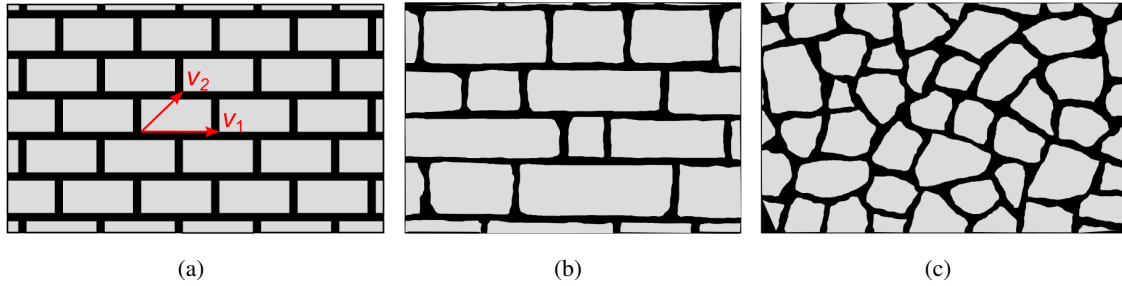


**Figure 1:** Masonry texture examples: (a) periodic, (b) quasi-periodic, (c) chaotic.

For this reason, alternative smeared continuum formulations have also been developed. For periodic masonry, early contributions include those of [6] and [7]. A key development was to use a unit cell or representative volume element (RVE) to ensure the specific properties of masonry can be properly represented. For non-periodic masonry, [8] used RVEs in conjunction with ‘test-windows’ of increasing dimensions to capture the elastic properties of the masonry, later extended to enable the strength of the masonry element to be determined [9].

In this paper the Discontinuity Layout Optimization (DLO) numerical limit analysis is employed to compare the in-plane load carrying capacities of periodic and non-periodic masonry elements. Unlike with finite elements, DLO [10] allows singularities in stress or displacements to be handled in a direct and natural manner, without the need of tailored meshes or mesh refinement.

## 2 NON PERIODIC MASONRY CLASSIFICATION

A first classification, has been presented as follows [11]:

- a **periodic texture**, made of equal blocks arranged according to a periodic pattern;
- a **quasi-periodic texture**, where the blocks can have different width and height but are arranged such that horizontal courses can be identified, whereas vertical mortar joints are randomly positioned;
- a **chaotic texture**, where the blocks have different width and height and are arranged without any clear pattern. It is possible that some vertical joints are aligned.

An example of these texture typologies is shown in Figure 2. It is worth noting that, in the case of chaotic texture, the blocks have been reduced to rectangles in order to simplify the analysis and the future realization of experimental tests. In all cases the heights of the blocks are equal, which is not true in general, but again this is to facilitate experimental tests on sample walls, realized with half height UNI brick (with no holes) [12]. Moreover, in this work, a further classification for non-periodic masonry is presented, with a particular focus on quasi periodic textures. While the classification of a periodic texture is straightforward, the classification of an irregular texture is not easy and univocal. For this reason a simple algorithm is presented.

Once the periodicity is excluded, the first thing is to check the horizontality of the mortar bed joints; if this is not fulfilled then the texture can be taken to be chaotic, otherwise the texture is quasi-periodic.

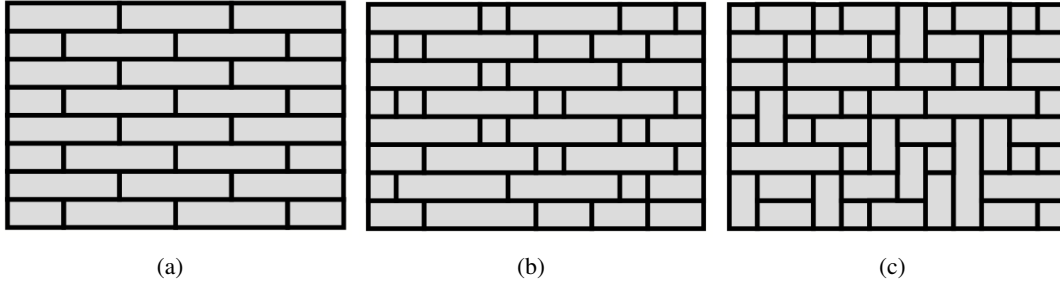


**Figure 2:** Masonry texture examples: (a) periodic, (b) quasi-periodic, (c) chaotic.

The following step is to provide a parameter to describe the degree of bonding between the courses and so the key idea of vertical minimum length path across the panel used in [13] is chosen and properly modified for our purpose.

The paths of minimum length along mortar joints are drawn, starting from the top to the bottom (red lines) and the other way around (blue lines), as in Fig. 3(a) and the mean value of these paths ( $p_i$ ) is evaluated. Priority is given to the descending paths since the upper part is more representative for the failure mechanism.

Then the mean aspect ratio (defined as the mean of the aspect ratios of each element) is evaluated and a corresponding periodic masonry structure having the same mean aspect ratio is considered. In the end, the length of the path ( $p_p$ ) for the periodic masonry is evaluated as in Equation 1:

$$p_p = H + \left( \frac{H}{h} - 1 \right) \cdot \frac{w}{2} \quad (1)$$

with  $H$ ,  $w$  and  $h$  defined in Fig. 3(b). If the dimensions of the elements are small compared to the wall size the formula becomes:

$$p_p = H \cdot \left( 1 + \frac{AR}{2} \right) \quad (2)$$

These formulas have been derived by simple geometrical observations and by combining the concepts of aspect ratio and minimum path length; hence they cannot be found in the current literature.

Then the value  $p$  is evaluated, defined as the ratio of  $p_i$  and  $p_p$ . This value is used to make a distinction between an Irregular Bond (IB) and a Stretcher Bond (SB). If the value is far from 1 (e.g. lower than 0.8) it means that the vertical mortar joints are almost aligned; otherwise elements are well staggered and we are close to a Stretcher Bond.

Finally, the coefficient of variation of the heights of the courses is evaluated ( $v$ ) and it provides a threshold between Similar height Stretcher Bond (SSB) and a Different height Stretcher Bond (DSB).

### 3 DISCONTINUITY LAYOUT OPTIMIZATION

In this section the key aspect of the DLO method are explained in order to provide essential details of the formulation.

DLO is an upper bound limit analysis approach and that involves the analysis of a network of potential discontinuities obtained connecting points on a grid. The problem obtained can be solved by Linear

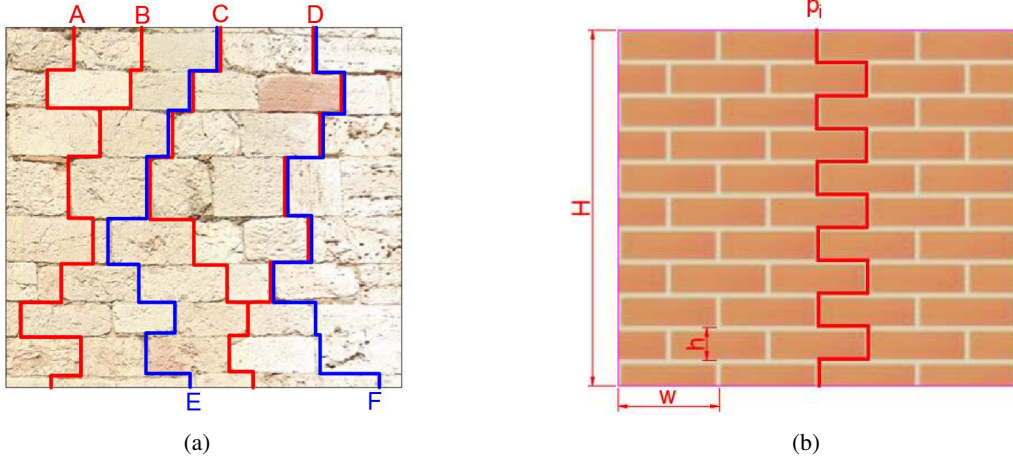


**Figure 3:** Evaluation of the paths through masonry: (a) shortest paths for a portion of irregular masonry; (b) path for corresponding periodic texture with the same mean aspect ratio

Programming and for a problem involving rigid blocks rotations [14] can be stated as follows:

$$\min_{\mathbf{d}, \mathbf{p}} \quad \lambda \mathbf{f}_L^T \mathbf{d} = -\mathbf{f}_D^T \mathbf{d} + \mathbf{g}^T \mathbf{p} \quad (3a)$$

$$\text{s.t.} \quad \mathbf{B} \mathbf{d} = \mathbf{0} \quad (3b)$$

$$\mathbf{N} \mathbf{p} - \mathbf{d} = \mathbf{0} \quad (3c)$$

$$\mathbf{f}_L^T \mathbf{d} = 1 \quad (3d)$$

$$\mathbf{p} \geq \mathbf{0} \quad (3e)$$

where  $\lambda$  is the live load factor,  $\mathbf{d}$  is a vector of relative displacement jumps (in this case it considering shear and normal displacements, and rotations),  $\mathbf{p}$  is a vector containing the plastic multipliers,  $\mathbf{g}$  is a vector of energy dissipation coefficients,  $\mathbf{f}_L^T$  and  $\mathbf{f}_D^T$  are respectively vectors of live and dead loads,  $\mathbf{B}$  is the global compatibility matrix and  $\mathbf{N}$  is the global flow rule matrix.

The compatibility condition has the following form for a given discontinuity  $i$ :

$$\mathbf{B}_i \mathbf{d}_i = \begin{bmatrix} \cos \theta_i & -\sin \theta_i & \frac{l_i \sin \theta_i}{2} \\ \sin \theta_i & \cos \theta_i & -\frac{l_i \cos \theta_i}{2} \\ 0 & 0 & 1 \\ -\cos \theta_i & \sin \theta_i & \frac{l_i \sin \theta_i}{2} \\ -\sin \theta_i & -\cos \theta_i & -\frac{l_i \cos \theta_i}{2} \\ 0 & 0 & -1 \end{bmatrix} \begin{bmatrix} s_i \\ n_i \\ \omega_i \end{bmatrix} \quad (4)$$

where  $\theta_i$  is the inclination of the  $i$ -th discontinuity with the  $x$ -axis,  $l_i$  is the length of the discontinuity, and  $\{s_i, n_i, \omega_i\}$  is the vector  $\mathbf{d}_i$  containing respectively the relative shear displacement, normal displacement and rotation. For the sake of clarity it is specified that for convenience the terms ‘energy dissipation’ and ‘displacement’ are used as shorthand for ‘rate of energy dissipation’ and ‘displacement rate’ respectively.

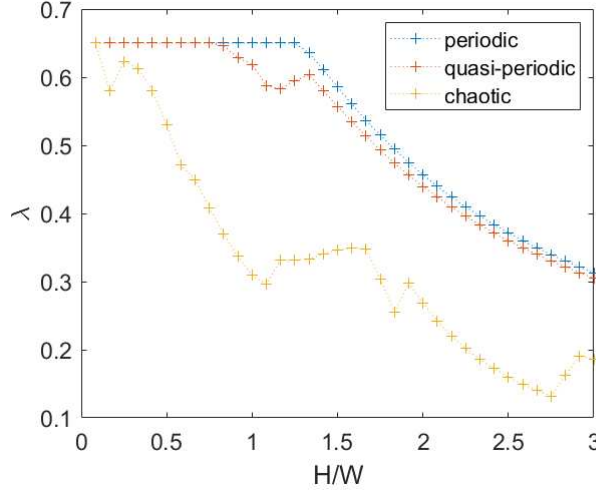


**Figure 4:** Comparison of failure multiplier at  $q = 0$  for different textures (averaging the response to left- and right-oriented forces for quasi-periodic and chaotic textures).

For the flow rule condition a Mohr-Coulomb criterion with associative friction is adopted, which has the following form for discontinuity  $i$  in the case of rigid rotations:

$$\mathbf{N}_i \mathbf{p}_i - \mathbf{d}_i = \begin{bmatrix} 1 & -1 & 0 & 0 \\ \tan \varphi_i & \tan \varphi_i & \frac{1}{2}l_i & \frac{1}{2}l_i \\ 0 & 0 & 1 & -1 \end{bmatrix} \begin{bmatrix} p_i^1 \\ p_i^2 \\ p_i^3 \\ p_i^4 \end{bmatrix} - \begin{bmatrix} s_i \\ n_i \\ \omega_i \end{bmatrix} = 0 \quad (5)$$

## 4 PARAMETRIC ANALYSIS

### 4.1 Variation with the height of the panel

The three different configurations of masonry described in the first part of Sec. 2 are now considered. For each, the variation of the load multiplier,  $\lambda$ , with height/width ratio of the panel is evaluated. The outcome is shown in Fig. 4. The masonry units are considered as rigid elements whereas the mortar is described by the Mohr-Coulomb criterion adopting zero cohesion and a coefficient of friction of 0.65. This result, already presented in [11] when a vertical load is applied at the top of the panel, shows that the periodic texture has the best load carrying capacity. The left hand side of the plot for the periodic and quasi-periodic textures is characterized by an horizontal line and this shows that for that H/W ratio the mechanism is purely translational and so the load factor ( $\lambda$ ) is equal to the tangent of the angle of friction. The quasi-periodic masonry has an irregular plot for a range of H/W between 0.9 and 1.4, due to the presence of a local mechanism that involves just a part of the panel width. The chaotic texture instead has a very irregular plot as due to the presence of slender elements it is more likely that local mechanisms will occur.

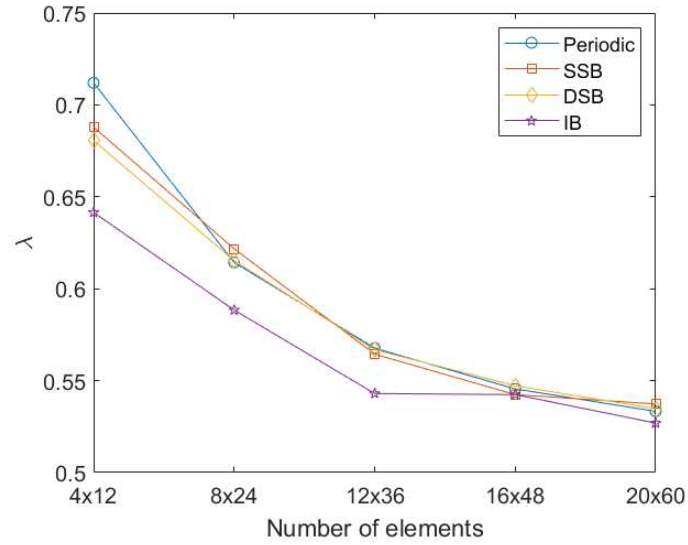


**Figure 5:** Horizontal loading on plane masonry walls: Parametric analysis. Comparison between textures for a rigid block analysis with associative friction. SSB = Similar height Stretcher Bond texture DSB = Different height Stretcher Bond texture IB = Irregular Bond texture

#### 4.2 Variation for the quasi-periodic texture for a square panel

In this section square panels having a different number of elements and different quasi-periodic textures are generated through a script and outcomes for the rigid block DLO analyses are shown. The local aspect ratio (i.e. the mean ratio between the height and the width of the elements) is fixed and equal to 3. For each number of elements and for each texture, five samples are generated and the outcomes for both right oriented and left oriented seismic actions are evaluated. Results are shown in Fig. 5, where in the  $y$ -axis the load factor is shown and in the  $x$ -axis the number of the elements varies in steps from 4x12 to 20x60. It can be observed that for a low number of elements the texture has a great influence whereas for a high number of elements the influence becomes negligible. Moreover the Irregular Bond texture (IB) shows the worst carrying capacity, while the the SSB and DSB outcome is close to the periodic one. This shows that exchanging the height of the courses has an effect that is mitigated when the mean of several samples is evaluated.

### 5 CONCLUSIONS

In this work the effect of masonry texture on the load carrying capacity of non-periodic masonry walls subjected to seismic actions is investigated.

Firstly, for periodic, quasi-periodic and chaotic textures it is found that when the height of the panel increases the chaotic texture has the lowest load carrying capacity, due to the presence of vertically aligned elements and the lack of horizontal courses.

A further classification for quasi-periodic masonry has been proposed to show the influence on texture for square panels of fixed mean local aspect ratio (i.e. relating to the shape of the masonry units). The

---

analyses undertaken shows that walls constructed with an Irregular Bond (IB) texture have the lowest load carrying capacity due to the alignment of vertical mortar joints.

This is ongoing work and a new homogenized DLO formulation is currently being applied to these types of walls to evaluate whether it can be applied to non-periodic textures and also whether it is computationally efficient as compared to the rigid block DLO formulation described herein.

## 6 ACKNOWLEDGEMENTS

Matthew Gilbert, Colin Smith and Linwei He acknowledge the financial support provided by the Engineering and Physical Sciences Research Council (EPSRC) under grant reference EP/T001305/1.

## REFERENCES

- [1] Falsone, G. and Lombardo, M., Stochastic representation of the mechanical properties of irregular masonry structures. *International Journal of Solids and Structures* (2007) **44**:8600-8612.
- [2] Livesley, R.K., Limit analysis of structures formed from rigid blocks. *International Journal for Numerical Methods in Engineering* (1978) **12**:1853–1871.
- [3] Baraldi, D. and Cecchi, A., Discrete approaches for the nonlinear analysis of in plane loaded masonry walls: Molecular dynamic and static algorithm solutions. *European Journal of Mechanics, A/Solids* (2016) **57**:165-177.
- [4] Ferris, M.C. and Tin-Loi, F., Limit analysis of frictional block assemblies as a mathematical program with complementarity constraints. *International Journal of Mechanical Sciences* (2001) **43**:209–224.
- [5] Gilbert, M and Casapulla, C and Ahmed, H.M., Limit analysis of masonry block structures with non-associative frictional joints using linear programming. *Computers and Structures* (2001) **84**:873–887.
- [6] Pande, G.N. and Liang, J.X. and Middleton, J., Equivalent elastic moduli for brick masonry. *Computers and Geotechnics* (1989) **8**:243-265.
- [7] Anthoine, A., Derivation of the in-plane elastic characteristics of masonry through homogenization theory. *International Journal of Solids and Structures* (1995) **32**:137-163.
- [8] Cluni, F. and Gusella V., Homogenization of non-periodic masonry structures. *International Journal of Solids and Structures* (2004) **41**:1911-1923.
- [9] Cavalagli, N. and Cluni, F. and Gusella, V., Strength domain of non-periodic masonry by homogenization in generalized plane state. *European Journal of Mechanics - A/Solids* (2011) **30**:113-126.
- [10] Smith, C. and Gilbert, M., Application of discontinuity layout optimization to plane plasticity problems. *Proc. R. Soc. A* (2007) **463**:2461-2484.
- [11] Schiantella, M. and Cluni, F. and Gusella, V., Parametric Analysis of Failure Loads of Masonry Textures by Means of Discontinuity Layout Optimization (DLO). *Materials* (2022) **15**:art. 3691.

- 
- [12] Cluni, F. and Gusella V. and Vinti, G., Masonry elastic characteristics assessment by thermographic images. *Meccanica* (2019) **54**:1339-1349.
- [13] Borri, A. and Corradi M. and De Maria, A., The Failure of Masonry Walls by Disaggregation and the Masonry Quality Index. *Heritage* (2020) **3**:1162–1198.
- [14] Gilbert, M. and Smith, C.C. and Pritchard, T.J., Masonry arch analysis using discontinuity layout optimisation. *Proceedings of the Institution of Civil Engineers: Engineering and Computational Mechanics* (2010) **3**:155-166.